Available online at www.sciencedirect.com
ScienceDirect
Journal of Sound and Vibration 324 (2009) 962–982
JOURNAL OF SOUND AND VIBRATION
www.elsevier.com/locate/jsvi

Nonlinear vibration of edge cracked functionally graded Timoshenko beams

S. Kitipornchai[a], L.L. Ke[a,c], J. Yang[b,*], Y. Xiang[d]

[a]*Department of Building and Construction, City University of Hong Kong, Hong Kong*
[b]*School of Aerospace, Mechanical and Manufacturing Engineering, RMIT University, PO Box 71, Bundoora, Victoria 3083, Australia*
[c]*Institute of Solid Mechanics, Beijing Jiao Tong University, 100044 Beijing, PR China*
[d]*School of Engineering, University of Western Sydney, Penrith South, NSW 1797, Australia*

Received 16 September 2008; received in revised form 10 February 2009; accepted 21 February 2009
Handling Editor: L.G. Tham
Available online 20 March 2009

Abstract

Nonlinear vibration of beams made of functionally graded materials (FGMs) containing an open edge crack is studied in this paper based on Timoshenko beam theory and von Kármán geometric nonlinearity. The cracked section is modeled by a massless elastic rotational spring. It is assumed that material properties follow exponential distributions through beam thickness. The Ritz method is employed to derive the governing eigenvalue equation which is then solved by a direct iterative method to obtain the nonlinear vibration frequencies of cracked FGM beams with different end supports. A detailed parametric study is conducted to study the influences of crack depth, crack location, material property gradient, slenderness ratio, and end supports on the nonlinear free vibration characteristics of cracked FGM beams. It is found that unlike isotropic homogeneous beams, both intact and cracked FGM beams show different vibration behavior at positive and negative amplitudes due to the presence of bending–extension coupling in FGM beams.

1. Introduction

The dynamic characteristics of cracked structures are of considerable importance in structural health monitoring. It is known that a crack in a structure introduces a local flexibility, reduces the stiffness and may change the dynamic behavior of the structure. The linear and nonlinear dynamic responses of homogeneous cracked structures have been extensively studied. Based on the line–spring model, many investigators [1–17] considered the linear free vibration and crack identification technique of cracked beams. Lee and Lim [18] developed a numerical method based on the Rayleigh method for predicting the natural frequencies of a rectangular plate with a centrally located crack. Khadem and Rezaee [19,20] studied the free vibration of a simply supported plate with an all-over crack or a finite length crack by using an analytical approach. Douka et al. [21] and Hadjileontiadis and Douka [22] presented the crack identification technique for plate structures based on wavelet analysis and kurtosis analysis. Rucka and Wilde [23] applied continuous wavelet transform

*Corresponding author. Tel.: +61 3 9925 6169; fax: +61 3 9925 6082.
E-mail address: j.yang@rmit.edu.au (J. Yang).

0022-460X/$ - see front matter © 2009 Elsevier Ltd. All rights reserved.
doi:10.1016/j.jsv.2009.02.023

to vibration based damage detection problems in beams and plates. Demir and Mermertas [24] obtained the natural frequencies of annular plates with circumferential cracks by using finite element method. El Bikri et al. [25] investigated the geometrically nonlinear free vibrations of a clamped–clamped beam with an edge crack. By using the Galerkin method, the dynamic instability and nonlinear response of the cracked plates subjected to period in-plane load were theoretically analyzed by Wu and Shih [26].

Functionally graded materials (FGMs) are inhomogeneous composites characterized by smooth and continuous variations in both compositional profile and material properties and have found a wide range of applications in many industries. In the past 10 years, many investigators have studied the linear [27–31] and nonlinear [32–37] dynamic responses of FGM structures. However, very limited literature is available concerning the effect of crack defects on the dynamic behavior of FGM structures. Sridhar et al. [38] developed an effective pseudo-spectral finite element method for wave propagation analysis in anisotropic and inhomogeneous structures with or without vertical and horizontal cracks. They also demonstrated the effectiveness of modulated pulse in detecting small cracks in composites and FGMs. Briman and Byrd [39] examined free and forced vibration of a functionally graded cantilever beam with damages such as a region with degraded stiffness adjacent to the root of the beam, a single delamination crack, and a single crack at the root cross-section of the beam propagating in the thickness direction. Most recently, Yang and Chen [40] analytically discussed the influence of open edge cracks on the vibration and buckling of Euler–Bernoulli FGM beams with different boundary conditions. They also studied the free and forced vibration of cracked Euler–Bernoulli inhomogeneous beams under an axial force and a transverse moving load [41]. Ke et al. [42] considered the free vibration and elastic buckling of cracked Timoshenko graded beam. However, all the aforementioned works for cracked FGM structures are limited to linear analysis only. To the best of authors' knowledge, no previous work has been done on the nonlinear vibration of the cracked FGM structures.

In this paper, the nonlinear vibration of FGM beams containing an open edge crack is studied based on von Kármán geometric nonlinearity. The effects of the transverse shear deformation and rotary inertia are considered within the framework of Timoshenko beam theory. The crack is modeled by a massless elastic rotational spring. The material properties of an FGM beam vary exponentially along the thickness direction. The Ritz method and a direct iterative technique are employed to obtain the nonlinear frequencies and mode shapes of cracked FGM beams with different end supports. Comprehensive numerical results are provided to examine the effects of material property gradient, crack depth, crack location, slenderness ratio, and boundary conditions on the nonlinear free vibration characteristics of the FGM beams.

2. The rotational spring model

Fig. 1a shows an FGM Timoshenko beam of length L and thickness h, containing an edge crack of depth a located at a distance L_1 from the left end. Its Young's modulus $E(z)$ and mass density $\rho(z)$ follow exponential distributions through thickness direction

$$E(z) = E_0\, e^{\beta z}, \quad \rho(z) = \rho_0\, e^{\beta z}, \tag{1}$$

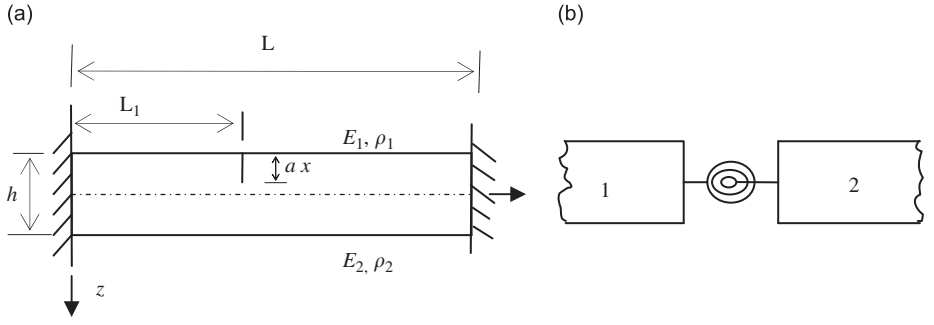

Fig. 1. (a) An FGM Timoshenko beam with an open edge crack and (b) rotational spring model.

where E_0 and ρ_0 are the values of Young's modulus and mass density at the midplane ($z=0$); β the constant characterizing the gradual variation of material properties along beam thickness, and $\beta=0$ corresponds to an isotropic homogeneous beam. Poisson's ratio v is taken to be constant since its influence on the stress intensity factors (SIFs) is quite limited [43].

It is assumed that the crack is perpendicular to beam surface and always remains open. The edge crack in a Timoshenko beam creates discontinuities in bending slope as well as transverse displacement at the cracked section. Since previous studies [6,9] showed that compared with the discontinuity in bending slope (mode I fracture), the discontinuity in transverse displacement (mode II fracture) has a much smaller contribution to system's total strain energy, the effect of mode II fracture is neglected in the present analysis. The crack section is therefore modeled as a massless elastic rotational spring shown in Fig. 1b. Based on this model, the cracked beam can be regarded as two sub-beams connected by the rotational spring at the cracked section whose bending stiffness is given as

$$K_T=\frac{1}{G}, \tag{2}$$

where G is the flexibility due to the crack and can be derived as [44]

$$\frac{(1-v^2)K_1^2}{E(a)}=\frac{M^2}{2}\frac{\mathrm{d}G}{\mathrm{d}a}, \tag{3}$$

where M is the bending moment at the cracked section, K_1 the SIF under mode I bending load, and $E(a)$ is Young's modulus at the crack tip.

The magnitude of SIF can be obtained from the data given by Erdogan and Wu [43] through Lagrange interpolation technique

$$K_1=\frac{6M\sqrt{\pi h\varsigma}}{h^2}F(\varsigma),\quad \varsigma=\frac{a}{h}\quad(\varsigma\leqslant 0.7), \tag{4}$$

where $\varsigma\leqslant 0.7$ implies that this paper considers crack depth ratio from 0.0 to 0.7 only, and

$$F(\varsigma)=1.910-2.752\varsigma-4.742\varsigma^2+146.776\varsigma^3-770.750\varsigma^4+1947.830\varsigma^5 -2409.170\varsigma^6+1177.980\varsigma^7,\quad \text{when } E_2/E_1=0.2, \tag{5a}$$

$$F(\varsigma)=1.150-1.662\varsigma+21.667\varsigma^2-192.451\varsigma^3+909.375\varsigma^4-2124.310\varsigma^5 +2395.830\varsigma^6-1031.750\varsigma^7,\quad \text{when } E_2/E_1=1.0, \tag{5b}$$

$$F(\varsigma)=0.650-0.859\varsigma+12.511\varsigma^2-72.627\varsigma^3+267.910\varsigma^4-535.236\varsigma^5 +545.139\varsigma^6-211.706\varsigma^7,\quad \text{when } E_2/E_1=5.0. \tag{5c}$$

The expression of $F(\varsigma)$ for other values of Young's modulus ratio can be obtained by using Lagrange interpolation technique as well. Substituting Eq. (4) into Eq. (3) leads to

$$G=\int_0^{\varsigma}\frac{72\pi(1-v^2)\varsigma F^2(\varsigma)}{E(\varsigma h)h^2}\,\mathrm{d}\varsigma. \tag{6}$$

From Eqs. (2), (5) and (6), the bending stiffness of the cracked section can be determined.

3. Nonlinear vibration analysis

3.1. Energy functional of the cracked FGM beam

Based on Timoshenko beam theory, the displacements of an arbitrary point in the beam along the x- and z-axes, denoted by $\tilde{U}(x,z,t)$ and $\tilde{W}(x,z,t)$, respectively, are

$$\tilde{U}(x,z,t)=U(x,t)+z\Psi(x,t),\quad \tilde{W}(x,z,t)=W(x,t), \tag{7}$$

where $U(x,t)$ and $W(x,t)$ are displacement components in the midplane, Ψ the rotation of beam cross-section and t the time. The von Kármán type nonlinear strain–displacement relations are given by

$$\varepsilon_x = \frac{\partial U}{\partial x} + z\frac{\partial \Psi}{\partial x} + \frac{1}{2}\left(\frac{\partial W}{\partial x}\right)^2, \quad \gamma_{xz} = \frac{\partial W}{\partial x} + \Psi. \tag{8}$$

The normal stress σ_{xx} and shear stress τ_{xz} are related to strains through linear elastic constitutive law as

$$\sigma_{xx} = Q_{11}(z)\left[\frac{\partial U}{\partial x} + z\frac{\partial \Psi}{\partial x} + \frac{1}{2}\left(\frac{\partial W}{\partial x}\right)^2\right], \quad \sigma_{xz} = Q_{55}(z)\left(\frac{\partial W}{\partial x} + \Psi\right), \tag{9}$$

where

$$Q_{11}(z) = \frac{E(z)}{1-\nu^2}, \quad Q_{55}(z) = \frac{E(z)}{2(1+\nu)}. \tag{10}$$

From Eqs. (7)–(10), the kinetic energy T and potential energy V of the cracked FGM beam are expressed as

$$T = \frac{1}{2}\int_0^{L_1}\int_{-h/2}^{h/2}\rho\left[\left(\frac{\partial U_1}{\partial t} + z\frac{\partial \Psi_1}{\partial t}\right)^2 + \left(\frac{\partial W_1}{\partial t}\right)^2\right]\mathrm{d}z\,\mathrm{d}x + \frac{1}{2}\int_{L_1}^{L}\int_{-h/2}^{h/2}\rho\left[\left(\frac{\partial U_2}{\partial t} + z\frac{\partial \Psi_2}{\partial t}\right)^2 + \left(\frac{\partial W_2}{\partial t}\right)^2\right]\mathrm{d}z\,\mathrm{d}x, \tag{11}$$

$$\begin{aligned} V = {} & \frac{1}{2}\int_0^{L_1}\int_{-h/2}^{h/2}\left\{Q_{11}\left[\frac{\partial U_1}{\partial x} + z\frac{\partial \Psi_1}{\partial x} + \frac{1}{2}\left(\frac{\partial W_1}{\partial x}\right)^2\right]^2 + Q_{55}\left(\frac{\partial W_1}{\partial x} + \Psi_1\right)^2\right\}\mathrm{d}z\,\mathrm{d}x \\ & + \frac{1}{2}\int_{L_1}^{L}\int_{-h/2}^{h/2}\left\{Q_{11}\left[\frac{\partial U_2}{\partial x} + z\frac{\partial \Psi_2}{\partial x} + \frac{1}{2}\left(\frac{\partial W_2}{\partial x}\right)^2\right]^2 + Q_{55}\left(\frac{\partial W_2}{\partial x} + \Psi_2\right)^2\right\}\mathrm{d}z\,\mathrm{d}x + \frac{1}{2}K_t(\Delta\Psi)^2, \end{aligned} \tag{12}$$

where $\Delta\Psi = \Psi_2(L_1) - \Psi_1(L_1)$; subscript $i = 1,2$ in U_i, Ψ_i, W_i refer to the left sub-beam and right sub-beam divided by the crack. Note that the last term on the right-hand side of Eq. (12) denotes the potential energy due to the rotational spring.

Define the stiffness components and inertia related terms as

$$\{A_{11}, B_{11}, D_{11}\} = \int_{-h/2}^{h/2} Q_{11}(z)\{1, z, z^2\}\,\mathrm{d}z, \quad A_{55} = \int_{-h/2}^{h/2}\kappa Q_{55}(z)\,\mathrm{d}z, \quad \{I_1, I_2, I_3\} = \int_{-h/2}^{h/2}\rho(z)\{1, z, z^2\}\,\mathrm{d}z, \tag{13}$$

where $\kappa = 5/6$ is shear correction factor. Then, the maximum kinetic energy $T_{\max}$ of the cracked FGM beam undergoing harmonic motion can be written as

$$T_{\max} = \frac{\Omega^2}{2}\int_0^{L_1}(I_1U_1^2 + 2I_2U_1\Psi_1 + I_3\Psi_1^2 + I_1W_1^2)\,\mathrm{d}x + \frac{\Omega^2}{2}\int_{L_1}^{L}(I_1U_2^2 + 2I_2U_2\Psi_2 + I_3\Psi_2^2 + I_1W_2^2)\,\mathrm{d}x, \tag{14}$$

where Ω is the nonlinear frequency of the beam. If V_{linear} and $V_{\text{nonlinear}}$ denote the potential energy associated with the linear and nonlinear strain terms in Eq. (8), respectively, the maximum potential energy $V_{\max}$ of the cracked FGM beam is expressed as

$$V_{\max} = V_{\text{linear}} + V_{\text{nonlinear}}, \tag{15}$$

where

$$\begin{aligned} V_{\text{linear}} = {} & \frac{1}{2}\int_0^{L_1}\left[A_{11}\left(\frac{\partial U_1}{\partial x}\right)^2 + 2B_{11}\frac{\partial U_1}{\partial x}\frac{\partial \Psi_1}{\partial x} + D_{11}\left(\frac{\partial \Psi_1}{\partial x}\right)^2 + A_{55}\left(\frac{\partial W_1}{\partial x} + \Psi_1\right)^4\right]\mathrm{d}x \\ & + \frac{1}{2}\int_{L_1}^{L}\left[A_{11}\left(\frac{\partial U_2}{\partial x}\right)^2 + 2B_{11}\frac{\partial U_2}{\partial x}\frac{\partial \Psi_2}{\partial x} + D_{11}\left(\frac{\partial \Psi_2}{\partial x}\right)^2 + A_{55}\left(\frac{\partial W_2}{\partial x} + \Psi_2\right)^2\right]\mathrm{d}x + \frac{1}{2}K_t(\Delta\Psi)^2, \end{aligned} \tag{16}$$

$$V_{\text{nonlinear}} = \frac{1}{2}\int_0^{L_1}\left[A_{11}\frac{\partial U_1}{\partial x}\left(\frac{\partial W_1}{\partial x}\right)^2 + B_{11}\frac{\partial \Psi_1}{\partial x}\left(\frac{\partial W_1}{\partial x}\right)^2 + \frac{1}{4}A_{11}\left(\frac{\partial W_1}{\partial x}\right)^4\right]\mathrm{d}x + \frac{1}{2}\int_{L_1}^{L}\left[A_{11}\frac{\partial U_2}{\partial x}\left(\frac{\partial W_2}{\partial x}\right)^2 + B_{11}\frac{\partial \Psi_2}{\partial x}\left(\frac{\partial W_2}{\partial x}\right)^2 + \frac{1}{4}A_{11}\left(\frac{\partial W_2}{\partial x}\right)^4\right]\mathrm{d}x. \tag{17}$$

Introducing the following dimensionless quantities

$$\zeta = \frac{x}{L}, \quad \zeta_0 = \frac{L_1}{L}, \quad (u, w) = \frac{(U, W)}{h}, \quad (\bar{I}_1, \bar{I}_2, \bar{I}_3) = \left(\frac{I_1}{I_{10}}, \frac{I_2}{I_{10}h}, \frac{I_3}{I_{10}h^2}\right), \quad \psi = \Psi, \tag{18a}$$

$$\eta = \frac{L}{h}, \quad (a_{11}, a_{55}, b_{11}, d_{11}) = \left(\frac{A_{11}}{A_{110}}, \frac{A_{55}}{A_{110}}, \frac{B_{11}}{A_{110}h}, \frac{D_{11}}{A_{110}h^2}\right), \quad \omega = \Omega L\sqrt{\frac{I_{10}}{A_{110}}}, \tag{18b}$$

where A_{110} and I_{10} are the values of A_{11} and I_1 of a homogeneous beam (i.e., $\beta = 0$), Eqs. (14), (16) and (17) can be expressed in dimensionless form

$$T^*_{\max} = \frac{\omega^2}{2}\left[\int_0^{\zeta_0}(\bar{I}_1u_1^2 + 2\bar{I}_2u_1\psi_1 + \bar{I}_3\psi_1^2 + \bar{I}_1w_1^2)\,\mathrm{d}\zeta + \int_{\zeta_0}^{1}(\bar{I}_1u_2^2 + 2\bar{I}_2u_2\psi_2 + \bar{I}_3\psi_2^2 + \bar{I}_1w_2^2)\,\mathrm{d}\zeta\right], \tag{19}$$

$$V^*_{\text{linear}} = \frac{1}{2}\int_0^{\zeta_0}\left[a_{11}\left(\frac{\partial u_1}{\partial \zeta}\right)^2 + 2b_{11}\frac{\partial u_1}{\partial \zeta}\frac{\partial \psi_1}{\partial \zeta} + d_{11}\left(\frac{\partial \psi_1}{\partial \zeta}\right)^2 + a_{55}\left(\frac{\partial w_1}{\partial \zeta} + \eta\psi_1\right)^2\right]\mathrm{d}\zeta + \frac{1}{2}\int_{\zeta_0}^{1}\left[a_{11}\left(\frac{\partial u_2}{\partial \zeta}\right)^2 + 2b_{11}\frac{\partial u_2}{\partial \zeta}\frac{\partial \psi_2}{\partial \zeta} + d_{11}\left(\frac{\partial \psi_2}{\partial \zeta}\right)^2 + a_{55}\left(\frac{\partial w_2}{\partial \zeta} + \eta\psi_2\right)^2\right]\mathrm{d}\zeta + \frac{1}{2}K^*_T(\Delta\psi)^2, \tag{20}$$

$$V^*_{\text{nonlinear}} = \frac{1}{2}\int_0^{\zeta_0}\left[\frac{a_{11}}{\eta}\frac{\partial u_1}{\partial \zeta}\left(\frac{\partial w_1}{\partial \zeta}\right)^2 + \frac{b_{11}}{\eta}\frac{\partial \psi_1}{\partial \zeta}\left(\frac{\partial w_1}{\partial \zeta}\right)^2 + \frac{a_{11}}{4\eta^2}\left(\frac{\partial w_1}{\partial \zeta}\right)^4\right]\mathrm{d}\zeta + \frac{1}{2}\int_{\zeta_0}^{1}\left[\frac{a_{11}}{\eta}\frac{\partial u_2}{\partial \zeta}\left(\frac{\partial w_2}{\partial \zeta}\right)^2 + \frac{b_{11}}{\eta}\frac{\partial \psi_2}{\partial \zeta}\left(\frac{\partial w_2}{\partial \zeta}\right)^2 + \frac{a_{11}}{4\eta^2}\left(\frac{\partial w_2}{\partial \zeta}\right)^4\right]\mathrm{d}\zeta, \tag{21}$$

where

$$T^*_{\max} = \frac{T_{\max}}{\Delta_0}, \quad V^*_{\text{linear}} = \frac{V_{\text{linear}}}{\Delta_0}, \quad V^*_{\text{nonlinear}} = \frac{V_{\text{nonlinear}}}{\Delta_0}, \quad K^*_T = \frac{K_T}{\Delta_0}, \quad \Delta_0 = \frac{A_{110}h^2}{L}. \tag{22}$$

Therefore, the energy functional for the cracked Timoshenko beam can be written as

$$\Pi = V^*_{\text{linear}} + V^*_{\text{nonlinear}} - T^*_{\max}. \tag{23}$$

3.2. Ritz trial functions

The present study considers cracked FGM beams with three different end supports, i.e., hinged at both ends (H–H), clamped at both ends (C–C), or clamped at left end and hinged at right end (C–H). The automated Ritz method [45,46] is employed to derive the governing eigenvalue equation for nonlinear vibration of cracked FGM beams. The Ritz trial functions for each sub-beam are expressed in the form of

$$u_1(\zeta) = \sum_{j=1}^{N} A_j\zeta^j, \quad u_2(\zeta) = \sum_{j=1}^{N} \tilde{A}_j\zeta^{j-1}(1-\zeta), \tag{24a}$$

$$w_1(\zeta) = \sum_{j=1}^{N} B_j\zeta^j, \quad w_2(\zeta) = \sum_{j=1}^{N} \tilde{B}_j\zeta^{j-1}(1-\zeta), \tag{24b}$$

$$\psi_1(\zeta)=\begin{cases}\sum_{j=1}^{N} C_j\zeta^{j-1}, & \text{for hinged end,}\\ \sum_{j=1}^{N} C_j\zeta^{j}, & \text{for clamped end,}\end{cases}\qquad \psi_2(\zeta)=\begin{cases}\sum_{j=1}^{N} \tilde{C}_j\zeta^{j-1}, & \text{for hinged end,}\\ \sum_{j=1}^{N} \tilde{C}_j\zeta^{j-1}(1-\zeta), & \text{for clamped end,}\end{cases} \tag{24c}$$

where N is the total number of polynomial terms; A_j, B_j, C_j, $\tilde{A}_j$, $\tilde{B}_j$, $\tilde{C}_j$ are unknown coefficients.

For the cracked FGM beams, the compatibility conditions enforcing the continuity of axial displacement and transverse deflection at the cracked section are

$$u_1(\zeta_0)=u_2(\zeta_0),\quad w_1(\zeta_0)=w_2(\zeta_0), \tag{25}$$

and a jump in the rotation due to bending exists which requires

$$\psi_2(\zeta_0)-\psi_1(\zeta_0)=\frac{1}{K_T^*}\left(b_{11}\frac{\partial u_2}{\partial\zeta}+d_{11}\frac{\partial\psi_2}{\partial\zeta}\right)_{\zeta=\zeta_0}. \tag{26}$$

It should be pointed out that on the right-hand side of Eq. (26), linear bending moment is used as an approximation in order to avoid the nonlinear terms in trial functions. Note that the trial functions in Eq. (24) can satisfy the geometric boundary conditions on both ends but cannot satisfy the compatibility conditions given in Eqs. (25) and (26). In order to enforce the requirements given in Eqs. (25) and (26) at the cracked section, the trial functions $u_1(\zeta)$, $w_1(\zeta)$, and $\psi_1(\zeta)$ for the left sub-beam need to be modified based on Eqs. (25) and (26) while those for right sub-beam ($u_2(\zeta)$, $w_2(\zeta)$, and $\psi_2(\zeta)$) remain unchanged. The final forms of trial functions of the left sub-beams are expressed as follows:

$$u_1(\zeta)=u_a(\zeta)+u_b(\zeta),\quad w_1(\zeta)=w_a(\zeta)+w_b(\zeta),\quad \psi_1(\zeta)=\psi_a(\zeta)+\psi_b(\zeta)+\psi_c(\zeta), \tag{27}$$

where

$$u_a(\zeta)=\sum_{j=1}^{N} A_j\zeta^j(\zeta-\zeta_0),\quad u_b(\zeta)=\frac{\zeta}{\zeta_0}\sum_{j=1}^{N}\tilde{A}_j\zeta_0^{j-1}(1-\zeta_0), \tag{28}$$

$$w_a(\zeta)=\sum_{j=1}^{N} B_j\zeta^j(\zeta-\zeta_0),\quad w_b(\zeta)=\frac{\zeta}{\zeta_0}\sum_{j=1}^{N}\tilde{B}_j\zeta_0^{j-1}(1-\zeta_0), \tag{29}$$

$$\text{H}-\text{H beam}:\begin{cases}\psi_a(\zeta)=\sum_{j=1}^{N} C_j\zeta^{j-1}(\zeta-\zeta_0),\\ \psi_b(\zeta)=\sum_{j=1}^{N}\tilde{C}_j\left[\zeta_0^{j-1}-\frac{d_{11}}{K_T^*}(j-1)\zeta_0^{j-2}\right],\\ \psi_c(\zeta)=-\frac{b_{11}}{K_T^*}\sum_{j=1}^{N}\tilde{A}_j[(j-1)\zeta_0^{j-2}(1-\zeta_0)-\zeta_0^{j-1}],\end{cases} \tag{30a}$$

$$\text{C}-\text{C beam}:\begin{cases}\psi_a(\zeta)=\sum_{j=1}^{N} C_j\zeta^{j}(\zeta-\zeta_0),\\ \psi_b(\zeta)=\frac{\zeta}{\zeta_0}\sum_{j=1}^{N}\tilde{C}_j\left\{\zeta_0^{j-1}(1-\zeta_0)-\frac{d_{11}}{K_T^*}[(j-1)\zeta_0^{j-2}(1-\zeta_0)-\zeta_0^{j-1}]\right\},\\ \psi_c(\zeta)=-\frac{\zeta\, b_{11}}{\zeta_0 K_T^*}\sum_{j=1}^{N}\tilde{A}_j[(j-1)\zeta_0^{j-2}(1-\zeta_0)-\zeta_0^{j-1}],\end{cases} \tag{30b}$$

$$\text{C}-\text{H beam}: \begin{cases} \psi_a(\zeta) = \sum_{j=1}^{N} C_j \zeta^j (\zeta - \zeta_0), \\ \psi_b(\zeta) = \dfrac{\zeta}{\zeta_0}\left\{ \sum_{j=1}^{N} \tilde{C}_j \zeta_0^{j-1} - \dfrac{d_{11}}{K_T^*} \sum_{j=1}^{N} \tilde{C}_j (j-1)\zeta_0^{j-2} \right\}, \\ \psi_c(\zeta) = -\dfrac{\zeta}{\zeta_0} \dfrac{b_{11}}{K_T^*} \sum_{j=1}^{N} \tilde{A}_j [(j-1)\zeta_0^{j-2}(1-\zeta_0) - \zeta_0^{j-1}]. \end{cases} \tag{30c}$$

3.3. Solution technique

Substituting Eqs. (27)–(30) in to energy functional (23), and applying standard Ritz procedure to minimize the total energy functional with respect to the unknown coefficients

$$\frac{\partial \Pi}{\partial A_j} = 0, \quad \frac{\partial \Pi}{\partial \tilde{A}_j} = 0, \quad \frac{\partial \Pi}{\partial B_j} = 0, \quad \frac{\partial \Pi}{\partial \tilde{B}_j} = 0, \quad \frac{\partial \Pi}{\partial C_j} = 0, \quad \frac{\partial \Pi}{\partial \tilde{C}_j} = 0, \tag{31}$$

leads to nonlinear governing equation

$$([K_L] + \tfrac{1}{2}[K_{NL1}] + \tfrac{1}{3}[K_{NL2}])\{\mathrm{d}\} - \omega^2 [M]\{\mathrm{d}\} = 0, \tag{32}$$

where $\{\mathrm{d}\} = \{\{A_j\}^{\mathrm{T}}\ \{\tilde{A}_j\}^{\mathrm{T}}\ \{B_j\}^{\mathrm{T}}\ \{\tilde{B}_j\}^{\mathrm{T}}\ \{C_j\}^{\mathrm{T}}\ \{\tilde{C}_j\}^{\mathrm{T}}\}^{\mathrm{T}}$, $j = 1, 2, \ldots, N$; $[M]$ is the mass matrix, $[K_L]$ is the linear stiffness matrix, $[K_{NL1}]$ and $[K_{NL2}]$ are nonlinear stiffness matrices that are linear and quadratic functions in $\{\mathrm{d}\}$, respectively. $[K_L]$, $[K_{NL1}]$, $[K_{NL2}]$ and $[M]$ are $6N \times 6N$ symmetric matrices whose elements are given in Appendix A.

Before solving the nonlinear governing Eq. (32), we first examine the energy balance equation $V - T = 0$. It is noted that due to the bending–extension coupling effect in FGM beams (i.e., $B_{11} \neq 0$), Eq. (11) contains terms with odd powers such as $\partial \Psi_1/\partial x(\partial W_1/\partial x)^2$, $\partial \Psi_2/\partial x(\partial W_2/\partial x)^2$. This implies that when $\partial U_i/\partial t = \partial W_i/\partial t = \partial \Psi_i/\partial t = 0$ $(i = 1, 2)$, the energy balance equation does not yield equal and opposite roots. Thus, the FGM beam vibrates with different amplitudes at positive and negative cycles. Homogeneous beams, however, do not have bending–extension coupling effect and the energy balance equation produces equal and opposite roots. The similar phenomenon was observed for asymmetric cross-ply composite beams by Singh and Rao [47,48]. In fact, quite similar to asymmetric cross-ply composite beams, FGM beams have unsymmetrical through-thickness material property distribution as well. But, the material properties change continuously and smoothly in FGMs.

Based on the fact that the energy required in each deflection cycle is same, the nonlinear frequency of the cracked FGM beams can be obtained by computing the period of both positive and negative deflection cycles. The nonlinear free vibration problem in Eq. (32) can be solved by employing a direct iterative method described below:

Step 1. By neglecting the nonlinear matrices $[K_{NL1}]$ and $[K_{NL2}]$, a linear eigenvalue and the associated eigenvector are obtained from Eq. (32). The eigenvector is then appropriately scaled up such that the maximum transverse displacement is equal to a given vibration amplitude. At first, we assume the given amplitude is positive $w_{\max}$. Note that $w_{\max} = w(0.5)$ for clamped–clamped and hinged–hinged beams while $w_{\max} = w(0.55)$ for clamped–hinged beams.

Step 2. Using the eigenvector to calculate $[K_{NL1}]$ and $[K_{NL2}]$, a new eigenvalue and eigenvector are obtained from the updated eigensystem (32).

Step 3. The eigenvector is scaled up again and step 2 is repeated until the relative error between eigenvalues obtained from two consecutive iterations is within 0.1%. Then, the nonlinear half-cycle frequency ω_1 is obtained for the positive deflection cycle. Based on the amplitude and deformation in positive deflection cycle, the energy $V_{\max}^{+}$ can be computed from Eqs. (20) and (21).

Step 4. Given a negative vibration amplitude $w_{\min}$, repeat steps 1–3 to find the energy $V_{\max}^{-}$ in negative deflection cycle. If $V_{\max}^{+} = V_{\max}^{-}$, the nonlinear half-cycle frequency ω_2 is obtained for the negative deflection cycle; otherwise new values must be chosen for negative vibration amplitude and the

iteration procedure is continued till the new negative amplitude and deformation yield the same energy with that at positive amplitude.

The nonlinear half-cycle frequencies thus obtained give the periods Γ_1 and Γ_2 at positive and negative deflection cycles, i.e.,

$$\Gamma_1 = \frac{\pi}{\omega_1}, \quad \Gamma_2 = \frac{\pi}{\omega_2}, \tag{33}$$

Finally, the nonlinear frequency of the cracked FGM beams is computed as

$$\omega = \frac{2\pi}{\Gamma_1 + \Gamma_2}. \tag{34}$$

4. Numerical results

4.1. Convergence and comparison studies

Table 1 compares the linear fundamental frequencies of cracked FGM beams with varying total number of polynomial terms N in the trial functions. The parameters used in this example are $E_1 = 70\,\text{GPa}$, $v_1 = 0.33$, $\rho_1 = 2780\,\text{kg/m}^3$, $E_2/E_1 = 5$, $L/h = 6$, $a/h = 0.2$ and $L_1/L = 0.5$. E_1 and E_2 denote Young's modulus at the top and bottom surfaces of the beam, respectively. The analytical solutions given by Ke et al. [42] are also provided for direct comparison. It is seen that the accuracy of the present results is improved with an increasing number of polynomial terms and is monotonically convergent to analytical solutions at $N = 8$ or 10. Hence, $N = 8$ is used in all of the following numerical calculations.

Table 2 gives nonlinear frequency ratio ω_{nl}/ω_l at different maximum vibration amplitudes $W_{\max}/\Theta$ (= 1.0, 2.0, 3.0, 4.0, 5.0) for isotropic homogeneous hinged–hinged, clamped–clamped and clamped–hinged beams ($L/h = 100$, $h = 0.3\,\text{in}$). Here, $\Theta = \sqrt{I/h}$ is the radius of the gyration of the beam with I and A as the cross-section area and area moment of inertia, ω_{nl} and ω_l are the dimensionless nonlinear and linear frequencies, respectively. The present results agree very well with the finite element results obtained by Marur and Prathap [49].

Table 1
Linear fundamental frequency of cracked FGM beams ($E_2/E_1 = 5$, $L/h = 16$, $a/h = 0.2$, and $L_1/L = 0.5$).

N	H–H	C–C	C–H
2	0.18743	0.48367	0.27227
3	0.17681	0.36697	0.26148
5	0.17635	0.36487	0.25951
8	0.17635	0.36487	0.25933
10	0.17635	0.36487	0.25933
Ref. [42]	0.1760	0.3641	–

Table 2
Comparisons of nonlinear frequency ratio ω_{nl}/ω_l for isotropic homogeneous beams ($L/h = 100$ and $h = 0.3\,\text{in}$).

$W_{\max}/\Theta$	H–H		C–C		C–H	
	Present	Ref. [49]	Present	Ref. [49]	Present	Ref. [49]
1.0	1.11920	1.1181	1.03029	1.0300	1.05923	1.0595
2.0	1.41801	1.4178	1.11520	1.1147	1.21789	1.2193
3.0	1.80919	1.8094	1.24191	1.2420	1.44023	1.4448
4.0	2.24511	2.2455	1.39829	1.3987	1.69576	1.6720
5.0	2.70429	2.7052	1.57471	1.5751	1.94717	1.9088

Table 3 lists the dimensionless linear fundamental frequency ω_l for hinged–hinged and clamped–clamped FGM beams ($E_1 = 70\,\text{GPa}$, $v_1 = 0.33$, $\rho_1 = 2780\,\text{kg/m}^3$, $L/h = 6, 16$, $h = 0.1\,\text{m}$) with a centrally located open edge crack ($a/h = 0.2$, $L_1/L = 0.5$). Again, excellent agreement is achieved between the present results and analytical solutions [42].

It is mentioned above that Eq. (26) uses an approximation that the nonlinear term is excluded in the expression for bending moment. To address the error induced by this approximation, Table 4 presents the dimensionless nonlinear frequency ω_{nl} of the cracked hinged–hinged FGM beam obtained by the present Ritz method and differential quadrature method (DQM). The governing equations, boundary and compatibility

Table 3
Comparison of linear fundamental frequency of cracked FGM beams with $a/h = 0.2$ and $L_1/L = 0.5$.

L/h	E_2/E_1	H–H		C–C	
		Present	Ref. [42]	Present	Ref. [42]
16	0.2	0.17310	0.17279	0.36095	0.36018
	1.0	0.17222	0.1720	0.38475	0.3840
	5.0	0.17635	0.1760	0.36487	0.3641
6	0.2	0.41921	0.41415	0.82329	0.81249
	1.0	0.42454	0.4198	0.86882	0.8584
	5.0	0.43757	0.43231	0.83964	0.82893

Table 4
Comparison of the dimensionless nonlinear fundamental frequencies of hinged–hinged cracked FGM beams ($l/h = 6$, $a/h = 0.2$, and $L_1/L = 0.5$).

E_2/E_1	$w_{\max} = 0.2$		$w_{\max} = 0.4$	
	DQM	Present	DQM	Present
0.2	0.42893	0.43132 (0.55%)	0.46700	0.47796 (2.3%)
1.0	0.44985	0.45325 (0.75%)	0.51833	0.53042 (2.3%)
5.0	0.45061	0.45387 (0.72%)	0.52414	0.53383 (1.8%)

Table 5
Nonlinear frequency ratio ω_{nl}/ω_l for intact FGM beams ($l/h = 6$ and $h = 0.1\,\text{m}$).

Boundary condition	E_2/E_1	ω_l	$w_{\max}$				
			0.2	0.4	0.6	0.8	1.0
Hinged–hinged	0.2	0.45980	1.02173	1.11240	1.28512	1.51749	1.78919
	1.0	0.45214	1.07270	1.23172	1.47025	1.75054	2.05509
	5.0	0.45980	1.03234	1.20135	1.48610	1.79924	2.11749
Clamped–hinged	0.2	0.63836	1.02865	1.11008	1.23617	1.39309	1.55194
	1.0	0.66357	1.03266	1.12391	1.25896	1.42359	1.56858
	5.0	0.63836	1.03213	1.13268	1.28708	1.48872	1.64633
Clamped–clamped	0.2	0.86000	1.01926	1.07447	1.15936	1.26699	1.39057
	1.0	0.89912	1.01744	1.06764	1.14536	1.24455	1.35944
	5.0	0.86000	1.01926	1.07447	1.15936	1.26699	1.39057

conditions to be used in DQM solution process are given in Appendix B. The parameters used in this example are the same as in the first example. The figures in the brackets are the relative error between the results obtained by using the present method and DQM. It is found that the present results are very close to DQM ones, indicating that the approximation in Eq. (26) can give results with good accuracy.

Table 6
Effect of slenderness ratio L/h on the nonlinear frequency ratio ω_{nl}/ω_l of clamped–clamped FGM beams ($E_2/E_1 = 5.0$).

L/h	ω_1	w_{max}				
		0.2	0.4	0.6	0.8	1.0
6	0.86000	1.01926	1.07447	1.15936	1.26699	1.39057
12	0.48291	1.01681	1.06542	1.14094	1.23758	1.34998
24	0.24983	1.01629	1.06352	1.13729	1.23212	1.34307
40	0.15104	1.01622	1.06316	1.13659	1.23120	1.34190

Table 7
The nonlinear frequency ratio ω_{nl}/ω_l of cracked FGM beams ($l/h = 6$, $h = 0.1$ m, and $a/h = 0.2$).

Boundary condition	E_2/E_1	ω_1	w_{max}			
			0.2	0.4	0.6	0.8
Hinged–hinged	0.2	0.41921	1.02889	1.14014	1.33542	1.67698
	1.0	0.42454	1.06763	1.24940	1.50478	1.80428
	5.0	0.43757	1.03727	1.22001	1.51199	1.77428
Clamped–hinged	0.2	0.61861	1.03193	1.11799	1.25410	1.41598
	1.0	0.65025	1.03382	1.12803	1.26707	1.43522
	5.0	0.62881	1.03309	1.13513	1.29026	1.48647
Clamped–clamped	0.2	0.82329	1.02048	1.08000	1.17243	1.28806
	1.0	0.86882	1.01842	1.07133	1.15294	1.25704
	5.0	0.83964	1.01953	1.07557	1.16151	1.26965

Table 8
Nonlinear frequency ratio ω_{nl}/ω_l of cracked FGM beams with different crack depth ($l/h = 6$, $h = 0.1$ m, and $E_2/E_1 = 5.0$).

Boundary condition	a/h	ω_l	w_{max}			
			0.2	0.4	0.6	0.8
Hinged–hinged	0.1	0.45369	1.03475	1.20823	1.49145	1.75052
	0.2	0.43757	1.03727	1.22001	1.51199	1.77428
	0.3	0.41319	1.04364	1.24306	1.55343	1.79435
Clamped–hinged	0.1	0.63600	1.03245	1.13344	1.28763	1.48558
	0.2	0.62881	1.03309	1.13513	1.29026	1.48647
	0.3	0.61468	1.03446	1.13775	1.29611	1.49045
Clamped–clamped	0.1	0.85435	1.01937	1.07454	1.15955	1.26733
	0.2	0.83964	1.01953	1.07557	1.16151	1.26965
	0.3	0.81883	1.02005	1.07700	1.16491	1.2749

In what follows, Tables 5–8 and Figs. 2–6 present the solutions for nonlinear free vibration of hinged–hinged, clamped–clamped, and clamped–hinged FGM beams with or without an open edge crack. In Tables 5–8, the linear fundamental frequencies ω_l are also listed. Unless otherwise stated, the beam thickness $h = 0.1$ m, slenderness ratio $L/h = 6$, crack depth ratio $a/h = 0.1, 0.2, 0.3$, crack location $L_1/L = 0.5$, Young's

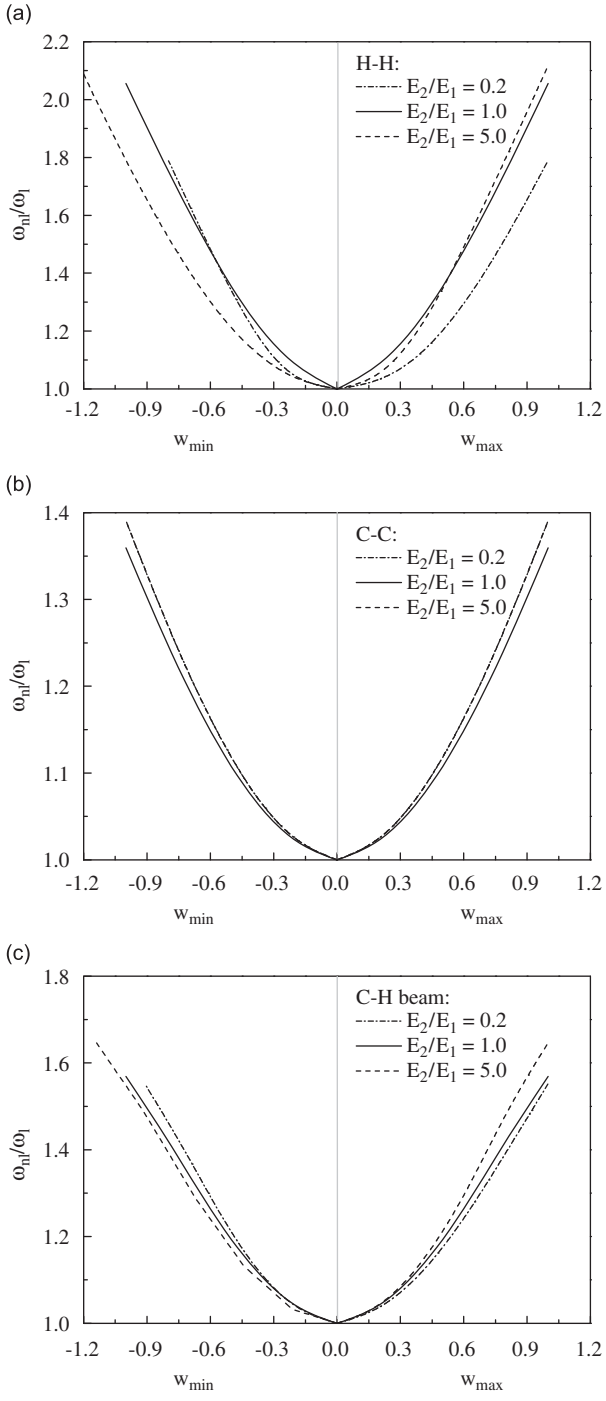

Fig. 2. Nonlinear frequency ratio versus amplitude curves for intact FGM beams: (a) hinged–hinged, (b) clamped–clamped, and (c) clamped–hinged.

modulus ratio $E_2/E_1 = 0.2, 1.0, 5.0$. As a special case, $E_2/E_1 = 1.0$ corresponds to an isotropic homogeneous beam. The top surface of the beam is 100% aluminum with material parameters $E_1 = 70\,\text{GPa}$, $v_1 = 0.33$, $\rho_1 = 2780\,\text{kg/m}^3$.

4.2. Nonlinear vibration of intact FGM beams

Table 5 gives the nonlinear frequency ratio ω_{nl}/ω_l for hinged–hinged, clamped–clamped and clamped–hinged intact FGM beams. All these beams exhibit a typical 'hard-spring' behavior, i.e., the nonlinear frequency ratio increases as the vibration amplitude is increased. It is noted that at $E_2/E_1 = 0.2$ and 5.0, the linear frequencies of beams with same end supports are the same. For nonlinear frequency ratios, however, this is true for clamped–clamped beams only but not for hinged–hinged and clamped–hinged beams. This is because the linear frequency is directly dependent on the value of d/I_1 (where $d = D_{11} - B_{11}^2/A_{11}$) which is almost identical at $E_2/E_1 = 0.2$ and 5.0. In nonlinear vibration analysis, only geometric boundary conditions are involved in clamped–clamped FGM beams while stress-related boundary conditions containing nonlinear terms need to be considered in both hinged–hinged and clamped–hinged FGM beams. As can be seen, an increase in Young's modulus ratio E_2/E_1 leads to a higher nonlinear frequency ratio when $w_{\max} \geqslant 0.6$ for hinged–hinged beam and when $w_{\max} \geqslant 0.4$ for clamped–hinged beam.

Table 6 shows the effect of slenderness ratio L/h on the linear frequency and nonlinear frequency ratio of clamped–clamped FGM beams ($E_2/E_1 = 5.0$). Both linear frequency and nonlinear frequency ratio decreases as slenderness ratio increases. As L/h changes from 6 to 40, the linear frequency drops remarkably but the nonlinear frequency ratio decreases slightly. For long FGM beams ($L/h \geqslant 12$), in particular, the effect of slenderness ratio on the nonlinear frequency ratio is very small and is negligible.

Fig. 2 plots the nonlinear frequency ratio versus dimensionless amplitude curves for FGM beams without edge crack. It is observed that at vibration amplitudes of same magnitude but opposite sign, frequency ratios of hinged–hinged and clamped–hinged graded beams ($E_2/E_1 = 0.2,\ 5.0$) are different, i.e., the curves are unsymmetrical. This is, as discussed before, due to the bending–stretching coupling effect that makes energy balance equation do not yields equal and opposite roots. However, for clamped–clamped beam and homogeneous beams, the nonlinear frequency ratio is independent of the sign of vibration amplitude and their curves are symmetrical.

4.3. Nonlinear vibration of cracked FGM beams

Table 7 tabulate the linear frequency and nonlinear frequency ratio ω_{nl}/ω_l for hinged–hinged, clamped–clamped and clamped–hinged FGM beams ($l/h = 6$, $h = 0.1\,\text{m}$, $a/h = 0.2$) with an open edge crack

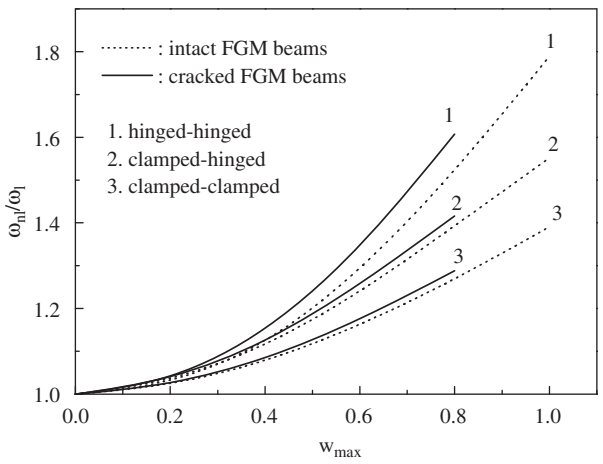

Fig. 3. Comparisons of nonlinear frequency ratio versus amplitude curves for intact and cracked FGM beams ($E_2/E_1 = 0.2$, $L/h = 6.0$, $a/h = 0.2$).

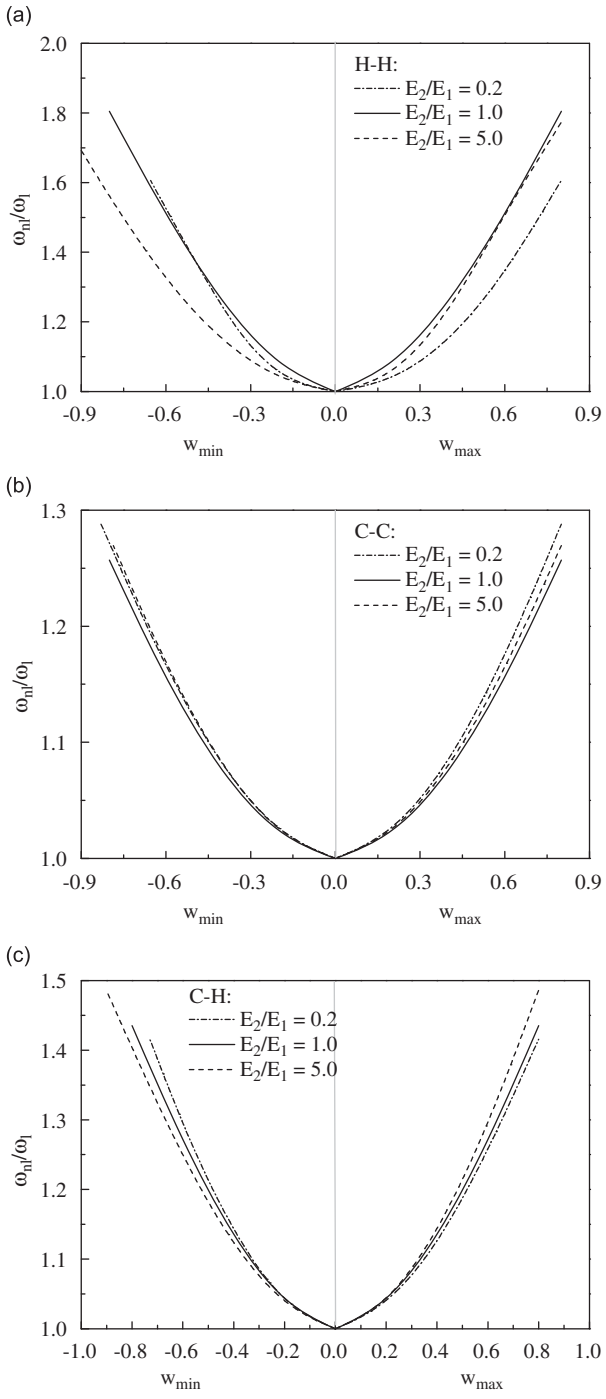

Fig. 4. Nonlinear frequency ratio versus amplitude curves for cracked FGM beams: (a) hinged–hinged, (b) clamped–clamped, and (c) clamped–hinged.

at the midpoint of the beam. All cracked FGM beams exhibit typical 'hard-spring' behavior. But unlike their intact counterparts, the cracked clamped–clamped beams with $E_2/E_1 = 0.2$ and 5.0 have different nonlinear frequency ratios at same vibration amplitude. The nonlinear frequency ratios of cracked hinged–hinged graded beams ($E_2/E_1 = 0.2$, 5.0) are significantly lower than that of the homogeneous beam ($E_2/E_1 = 1.0$)

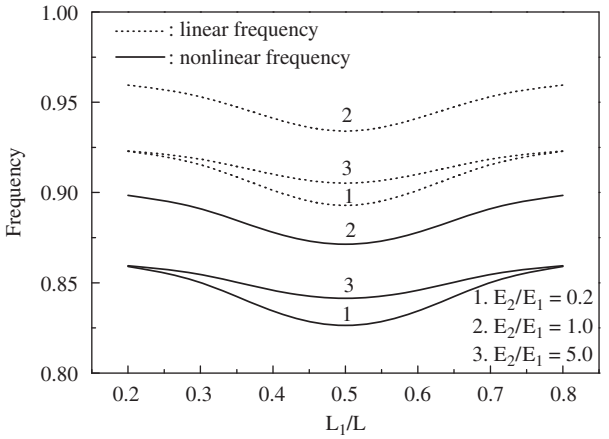

Fig. 5. Effect of crack location on linear and nonlinear frequencies of clamped–clamped cracked FGM beams ($l/h = 6$, $h = 0.1$ m, $a/h = 0.2$, $w_{max} = 0.4$).

while the clamped–clamped and clamped–hinged beams have the opposite behavior. The linear frequency is seen to be the maximum at $E_2/E_1 = 1.0$ for clamped–clamped and clamped–hinged beams but increase monotonically with increasing Young's modulus ratio E_2/E_1 for hinged–hinged beam. A comparison of the results in Tables 5 and 7 reveals that the linear frequencies of cracked FGM beams are lower than those of intact FGM beams.

The effect of the presence of an edge crack on the nonlinear vibration behavior is clearly depicted in Fig. 3 where the nonlinear frequency ratio versus vibration amplitude curves of FGM beams with and without an edge crack are directly compared. The nonlinear frequency ratio of a cracked FGM beam is higher than that of its intact counterpart. This effect is seen to be significant in a hinged–hinged beam but much less so in a clamped–clamped beam. This indicates that among the three boundary conditions considered in the present study, the hinged–hinged beam which has the lowest end supporting rigidity is most sensitive to edge crack.

Table 8 shows the effect of crack depth on the linear frequency and nonlinear frequency ratio ω_{nl}/ω_l of FGM beams ($E_2/E_1 = 5.0$, $l/h = 6$, $h = 0.1$ m). The deeper the edge crack is, the weaker the cracked section becomes. This leads to a smaller linear frequency but a slightly higher nonlinear frequency ratio at a given amplitude value.

Fig. 4 displays the effect of the sign of vibration amplitude on the nonlinear vibration behavior of cracked FGM beams. At vibration amplitudes of same magnitude but opposite sign, all cracked graded beams, including the clamped–clamped ones, have different nonlinear frequency ratios. This is quite different from the observations for intact clamped–clamped FGM beams although the difference between the nonlinear frequency ratios at positive and negative deflection cycles is not large for cracked clamped–clamped FGM beams. The nonlinear frequency ratio of cracked homogeneous beams, however, is still independent of the sign of vibration amplitude.

The effect of crack location on the linear and nonlinear fundamental frequencies of clamped–clamped FGM beams ($l/h = 6$, $h = 0.1$ m, $a/h = 0.2$, $w_{max} = 0.4$) is investigated in Fig. 5. It is found that both linear and nonlinear frequencies are most sensitive to crack located at the beam center. The influence of crack tends to be smaller as the crack is located closer to the beam ends. Compared with graded beams, the frequency of the homogeneous beam ($E_2/E_1 = 1.0$) is much more affected by the edge crack. The results for hinged–hinged and clamped–hinged beams are very similar to those of clamped–clamped beams and therefore, are not shown for brevity.

Fig. 6 gives nonlinear fundamental mode shapes for FGM beams with various crack depths ($a/h = 0.0$, 0.1, 0.2, 0.3) at $w_{max} = 0.6$. Note that $a/h = 0.0$ virtually indicates a beam without crack. The crack depth has insignificant effect on the nonlinear mode shape for clamped–hinged beam, but it is relative large for the hinged–hinged and clamped–clamped beams. It is found that the maximum amplitude occurs at the midpoint of the hinged–hinged and clamped–clamped beams but not for the clamped–hinged beam.

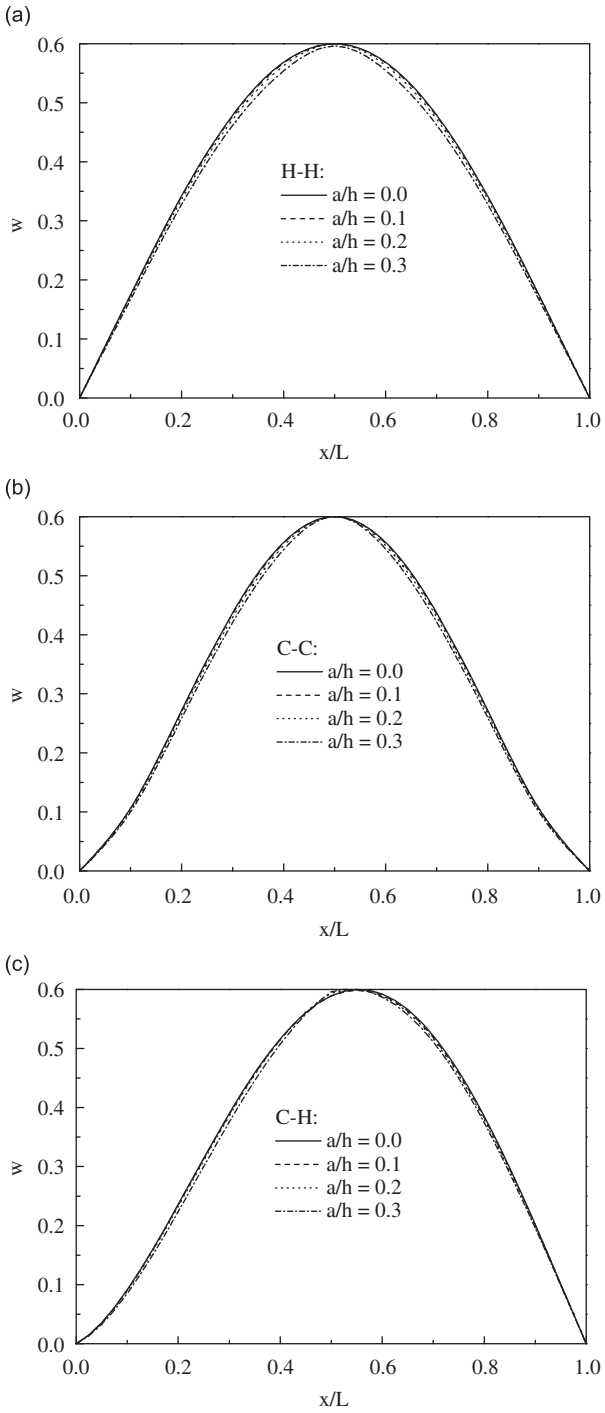

Fig. 6. Nonlinear mode shapes of FGM beams with different crack depth ($w_{max} = 0.6$): (a) hinged–hinged, (b) clamped–clamped, and (c) clamped–hinged.

5. Conclusions

The nonlinear vibration behavior of cracked FGM beams is studied within the framework of Timoshenko beam theory and von Kármán type displacement–strain relationship. The crack is modeled by a massless

elastic rotational spring. The materials properties are assumed to follow exponential distributions through thickness direction. The Ritz method and a direct iterative procedure are employed to find the nonlinear frequencies and associated mode shapes. The effects of material composition, crack depth, crack location, boundary conditions, and slenderness ratio on nonlinear free vibration characteristics of cracked FGM beams are studied in detail. Numerical results show that (1) all intact and cracked FGM beams exhibit typical 'hard-spring' behavior; (2) the nonlinear frequencies of the intact hinged–hinged and clamped–hinged graded beams are dependent on the sign of the vibration amplitudes; (3) at vibration amplitudes of same magnitude but opposite sign, nonlinear frequency ratios of all cracked graded beams are different although the difference is not significant for clamped–clamped graded beam; (4) the linear frequency is greatly reduced with an increase in crack depth but the nonlinear frequency ratio and mode shapes are much less affected by the change in crack depth; and (5) the linear and nonlinear frequencies of all beams are most sensitive to cracks located at the midpoint of the beam.

Acknowledgment

The work described in this paper was fully funded by a research grant from City University of Hong Kong (Project no. 7002211). The authors are grateful for this financial support.

Appendix A

Re-write trial functions in Eqs. (28)–(30) in the following form:

$$u_a(\zeta)=\sum_{j=1}^{N}A_j\Xi_{1j},\quad u_b(\zeta)=\sum_{j=1}^{N}\tilde{A}_j\Xi_{2j},\quad u_2(\zeta)=\sum_{j=1}^{N}\tilde{A}_j\Xi_{3j},\tag{A.1}$$

$$w_a(\zeta)=\sum_{j=1}^{N}B_j\Xi_{1j},\quad w_b(\zeta)=\sum_{j=1}^{N}\tilde{B}_j\Xi_{2j},\quad w_2(\zeta)=\sum_{j=1}^{N}\tilde{B}_j\Xi_{3j},\tag{A.2}$$

$$\psi_a(\zeta)=\sum_{j=1}^{N}C_j\Xi_{4j},\quad \psi_b(\zeta)=\sum_{j=1}^{N}\tilde{C}_j\Xi_{5j},\quad \psi_c(\zeta)=\sum_{j=1}^{N}\tilde{A}_j\Xi_{6j},\quad \psi_2(\zeta)=\sum_{j=1}^{N}\tilde{C}_j\Xi_{7j}.\tag{A.3}$$

The elements of symmetric linear stiffness matrix $[K_L]_{6N\times 6N}$ are

$$[K_L]_{(j,m)}=\int_0^{\zeta_0}a_{11}\frac{\partial\Xi_{1j}}{\partial\zeta}\frac{\partial\Xi_{1m}}{\partial\zeta}\,\mathrm{d}\zeta,\quad [K_L]_{(j,N+m)}=\int_0^{\zeta_0}\left(a_{11}\frac{\partial\Xi_{2j}}{\partial\zeta}+b_{11}\frac{\partial\Xi_{6j}}{\partial\zeta}\right)\frac{\partial\Xi_{1m}}{\partial\zeta}\,\mathrm{d}\zeta,$$

$$[K_L]_{(j,2N+m)}=[K_L]_{(j,3N+m)}=0,$$

$$[K_L]_{(j,4N+m)}=\int_0^{\zeta_0}b_{11}\frac{\partial\Xi_{4j}}{\partial\zeta}\frac{\partial\Xi_{1m}}{\partial\zeta}\,\mathrm{d}\zeta,\quad [K_L]_{(j,5N+m)}=\int_0^{\zeta_0}b_{11}\frac{\partial\Xi_{5j}}{\partial\zeta}\frac{\partial\Xi_{1m}}{\partial\zeta}\,\mathrm{d}\zeta,$$

$$[K_L]_{(N+j,N+m)}=\int_0^{\zeta_0}\left[b_{11}\left(\frac{\partial\Xi_{6j}}{\partial\zeta}\frac{\partial\Xi_{2m}}{\partial\zeta}+\frac{\partial\Xi_{2j}}{\partial\zeta}\frac{\partial\Xi_{6m}}{\partial\zeta}\right)+a_{11}\frac{\partial\Xi_{2j}}{\partial\zeta}\frac{\partial\Xi_{2m}}{\partial\zeta}+d_{11}\frac{\partial\Xi_{6j}}{\partial\zeta}\frac{\partial\Xi_{6m}}{\partial\zeta}+a_{55}\eta^2\Xi_{6j}\Xi_{6m}\right]\mathrm{d}\zeta$$
$$+\int_{\zeta_0}^{1}a_{11}\frac{\partial\Xi_{3j}}{\partial\zeta}\frac{\partial\Xi_{3m}}{\partial\zeta}\,\mathrm{d}\zeta+2K_T^*(\Xi_{6j}\Xi_{6m})_{\zeta=\zeta_0},$$

$$[K_L]_{(N+j,2N+m)}=\int_0^{\zeta_0}a_{55}\eta\frac{\partial\Xi_{1j}}{\partial\zeta}\Xi_{6m}\,\mathrm{d}\zeta,\quad [K_L]_{(N+j,3N+m)}=\int_0^{\zeta_0}a_{55}\eta\frac{\partial\Xi_{2j}}{\partial\zeta}\Xi_{6m}\,\mathrm{d}\zeta,$$

$$[K_L]_{(N+j,4N+m)}=\int_0^{\zeta_0}\left(b_{11}\frac{\partial\Xi_{4j}}{\partial\zeta}\frac{\partial\Xi_{2m}}{\partial\zeta}+d_{11}\frac{\partial\Xi_{4j}}{\partial\zeta}\frac{\partial\Xi_{6m}}{\partial\zeta}+a_{55}\eta^2\Xi_{4j}\Xi_{6m}\right)\mathrm{d}\zeta+2K_T^*(\Xi_{4j}\Xi_{6m})_{\zeta=\zeta_0},$$

$$[K_L]_{(N+j,5N+m)} = \int_0^{\zeta_0} \left(b_{11} \frac{\partial \Xi_{5j}}{\partial \zeta} \frac{\partial \Xi_{2m}}{\partial \zeta} + d_{11} \frac{\partial \Xi_{5j}}{\partial \zeta} \frac{\partial \Xi_{6m}}{\partial \zeta} + a_{55} \eta^2 \Xi_{5j} \Xi_{6m} \right) \mathrm{d}\zeta + \int_{\zeta_0}^{1} b_{11} \frac{\partial \Xi_{7j}}{\partial \zeta} \frac{\partial \Xi_{3m}}{\partial \zeta} \, \mathrm{d}\zeta + 2K_T^* \Xi_{6m} (\Xi_{5j} - \Xi_{7j})_{\zeta=\zeta_0},$$

$$[K_L]_{(2N+j,2N+m)} = \int_0^{\zeta_0} a_{55} \frac{\partial \Xi_{1j}}{\partial \zeta} \frac{\partial \Xi_{1m}}{\partial \zeta} \, \mathrm{d}\zeta, \quad [K_L]_{(2N+j,3N+m)} = \int_0^{\zeta_0} a_{55} \frac{\partial \Xi_{2j}}{\partial \zeta} \frac{\partial \Xi_{1m}}{\partial \zeta} \, \mathrm{d}\zeta,$$

$$[K_L]_{(2N+j,4N+m)} = \int_0^{\zeta_0} a_{55} \eta \Xi_{4j} \frac{\partial \Xi_{1m}}{\partial \zeta} \, \mathrm{d}\zeta,$$

$$[K_L]_{(2N+j,5N+m)} = \int_0^{\zeta_0} a_{55} \eta \Xi_{5j} \frac{\partial \Xi_{1m}}{\partial \zeta} \, \mathrm{d}\zeta, \quad [K_L]_{(3N+j,3N+m)} = \int_{\zeta_0}^{1} a_{55} \frac{\partial \Xi_{3j}}{\partial \zeta} \frac{\partial \Xi_{3m}}{\partial \zeta} \, \mathrm{d}\zeta + \int_0^{\zeta_0} a_{55} \frac{\partial \Xi_{2j}}{\partial \zeta} \frac{\partial \Xi_{2m}}{\partial \zeta} \, \mathrm{d}\zeta,$$

$$[K_L]_{(3N+j,4N+m)} = \int_0^{\zeta_0} a_{55} \eta \Xi_{4j} \frac{\partial \Xi_{2m}}{\partial \zeta} \, \mathrm{d}\zeta, \quad [K_L]_{(3N+j,5N+m)} = \int_{\zeta_0}^{1} a_{55} \eta \Xi_{7j} \frac{\partial \Xi_{3m}}{\partial \zeta} \, \mathrm{d}\zeta + \int_0^{\zeta_0} a_{55} \eta \Xi_{5j} \frac{\partial \Xi_{2m}}{\partial \zeta} \, \mathrm{d}\zeta,$$

$$[K_L]_{(4N+j,4N+m)} = \int_0^{\zeta_0} \left(d_{11} \frac{\partial \Xi_{4j}}{\partial \zeta} \frac{\partial \Xi_{4m}}{\partial \zeta} + a_{55} \eta^2 \Xi_{4j} \Xi_{4m} \right) \mathrm{d}\zeta + 2K_T^* (\Xi_{4j} \Xi_{4m})_{\zeta=\zeta_0},$$

$$[K_L]_{(4N+j,5N+m)} = \int_0^{\zeta_0} \left(d_{11} \frac{\partial \Xi_{5j}}{\partial \zeta} \frac{\partial \Xi_{4m}}{\partial \zeta} + a_{55} \eta^2 \Xi_{5j} \Xi_{4m} \right) \mathrm{d}\zeta + 2K_T^* (\Xi_{5j} \Xi_{5m} - \Xi_{7j} \Xi_{4m})_{\zeta=\zeta_0},$$

$$[K_L]_{(5N+j,5N+m)} = \int_{\zeta_0}^{1} \left(d_{11} \frac{\partial \Xi_{7j}}{\partial \zeta} \frac{\partial \Xi_{7m}}{\partial \zeta} + a_{55} \eta^2 \Xi_{7j} \Xi_{7m} \right) \mathrm{d}\zeta + \int_0^{\zeta_0} \left(d_{11} \frac{\partial \Xi_{5j}}{\partial \zeta} \frac{\partial \Xi_{5m}}{\partial \zeta} + a_{55} \eta^2 \Xi_{5j} \Xi_{5m} \right) \mathrm{d}\zeta + 2K_T^* (\Xi_{5j} \Xi_{5m} + \Xi_{7j} \Xi_{7m} - 2\Xi_{7j} \Xi_{5m})_{\zeta=\zeta_0}.$$

The elements of the symmetric mass matrix $[M]_{6N \times 6N}$ are

$$[M]_{(j,m)} = \int_0^{\zeta_0} \bar{I}_1 \Xi_{1j} \Xi_{1m} \, \mathrm{d}\zeta, \quad [M]_{(j,N+m)} = \int_0^{\zeta_0} (\bar{I}_1 \Xi_{2j} \Xi_{1m} + \bar{I}_2 \Xi_{6j} \Xi_{1m}) \, \mathrm{d}\zeta, \quad [M]_{(j,2N+m)} = [M]_{(j,3N+m)} = 0,$$

$$[M]_{(j,4N+m)} = \int_0^{\zeta_0} \bar{I}_2 \Xi_{4j} \Xi_{1m} \, \mathrm{d}\zeta, \quad [M]_{(j,5N+m)} = \int_0^{\zeta_0} \bar{I}_2 \Xi_{5j} \Xi_{1m} \, \mathrm{d}\zeta,$$

$$[M]_{(N+j,N+m)} = \int_{\zeta_0}^{1} \bar{I}_1 \Xi_{3j} \Xi_{3m} \, \mathrm{d}\zeta + \int_0^{\zeta_0} (\bar{I}_1 \Xi_{2j} \Xi_{2m} + \bar{I}_2 \Xi_{6j} \Xi_{2m} + \bar{I}_2 \Xi_{2j} \Xi_{6m} + \bar{I}_3 \Xi_{6j} \Xi_{6m}) \, \mathrm{d}\zeta,$$

$$[M]_{(N+j,2N+m)} = [M]_{(N+j,3N+m)} = 0, \quad [M]_{(N+j,4N+m)} = \int_0^{\zeta_0} (\bar{I}_2 \Xi_{4j} \Xi_{2m} + \bar{I}_3 \Xi_{4j} \Xi_{6m}) \, \mathrm{d}\zeta,$$

$$[M]_{(N+j,5N+m)} = \int_{\zeta_0}^{1} \bar{I}_2 \Xi_{7j} \Xi_{3m} \, \mathrm{d}\zeta + \int_0^{\zeta_0} (\bar{I}_2 \Xi_{5j} \Xi_{2m} + \bar{I}_3 \Xi_{5j} \Xi_{6m}) \, \mathrm{d}\zeta, \quad [M]_{(2N+j,2N+m)} = \int_0^{\zeta_0} \bar{I}_1 \Xi_{1j} \Xi_{1m} \, \mathrm{d}\zeta,$$

$$[M]_{(2N+j,3N+m)} = \int_0^{\zeta_0} \bar{I}_1 \Xi_{2j} \Xi_{1m} \, \mathrm{d}\zeta, \quad [M]_{(2N+j,4N+m)} = [M]_{(2N+j,5N+m)} = 0,$$

$$[M]_{(3N+j,3N+m)} = \int_{\zeta_0}^{1} \bar{I}_1 \Xi_{3j} \Xi_{3m} \, \mathrm{d}\zeta + \int_0^{\zeta_0} \bar{I}_1 \Xi_{2j} \Xi_{2m} \, \mathrm{d}\zeta, \quad [M]_{(3N+j,4N+m)} = [M]_{(3N+j,5N+m)} = 0,$$

$$[M]_{(4N+j,4N+m)} = \int_0^{\zeta_0} \bar{I}_3 \Xi_{4j} \Xi_{4m} \, \mathrm{d}\zeta, \quad [M]_{(4N+j,5N+m)} = \int_0^{\zeta_0} \bar{I}_3 \Xi_{5j} \Xi_{4m} \, \mathrm{d}\zeta,$$

$$[M]_{(5N+j,5N+m)} = \int_{\zeta_0}^{1} \bar{I}_3 \Xi_{7j} \Xi_{7m} \, \mathrm{d}\zeta + \int_0^{\zeta_0} \bar{I}_3 \Xi_{7j} \Xi_{5m} \, \mathrm{d}\zeta.$$

The elements of the nonlinear stiffness matrices $[K_{NL1}]_{6N\times 6N}$ and $[K_{NL2}]_{6N\times 6N}$ are

$$[K_{NL1}]_{(j,m)} = [K_{NL1}]_{(j,N+m)} = [K_{NL1}]_{(j,4N+m)} = [K_{NL1}]_{(j,5N+m)} = 0, \quad [K_{NL1}]_{(j,2N+m)} = \frac{a_{11}}{\eta} \int_0^{\zeta_0} \frac{\partial w_1}{\partial \zeta} \frac{\partial \Xi_{1j}}{\partial \zeta} \frac{\partial \Xi_{1m}}{\partial \zeta} \, \mathrm{d}\zeta,$$

$$[K_{NL1}]_{(j,3N+m)} = \frac{a_{11}}{\eta} \int_0^{\zeta_0} \frac{\partial w_1}{\partial \zeta} \frac{\partial \Xi_{2j}}{\partial \zeta} \frac{\partial \Xi_{1m}}{\partial \zeta} \, \mathrm{d}\zeta, \quad [K_{NL1}]_{(N+j,N+m)} = [K_{NL1}]_{(N+j,4N+m)} = [K_{NL1}]_{(N+j,5N+m)} = 0,$$

$$[K_{NL1}]_{(N+j,2N+m)} = \frac{1}{\eta} \int_0^{\zeta_0} \left(a_{11} \frac{\partial w_1}{\partial \zeta} \frac{\partial \Xi_{1j}}{\partial \zeta} \frac{\partial \Xi_{2m}}{\partial \zeta} + b_{11} \frac{\partial w_1}{\partial \zeta} \frac{\partial \Xi_{1j}}{\partial \zeta} \frac{\partial \Xi_{6m}}{\partial \zeta} \right) \mathrm{d}\zeta,$$

$$[K_{NL1}]_{(N+j,3N+m)} = \frac{a_{11}}{\eta} \int_{\zeta_0}^{1} \frac{\partial w_2}{\partial \zeta} \frac{\partial \Xi_{3j}}{\partial \zeta} \frac{\partial \Xi_{3m}}{\partial \zeta} \, \mathrm{d}\zeta + \frac{1}{\eta} \int_0^{\zeta_0} \frac{\partial w_1}{\partial \zeta} \frac{\partial \Xi_{2j}}{\partial \zeta} \left(a_{11} \frac{\partial \Xi_{2m}}{\partial \zeta} + b_{11} \frac{\partial \Xi_{6m}}{\partial \zeta} \right) \mathrm{d}\zeta,$$

$$[K_{NL1}]_{(2N+j,2N+m)} = [K_{NL1}]_{(2N+j,3N+m)} = 0, \quad [K_{NL1}]_{(2N+j,4N+m)} = \frac{b_{11}}{\eta} \int_0^{\zeta_0} \frac{\partial w_1}{\partial \zeta} \frac{\partial \Xi_{4j}}{\partial \zeta} \frac{\partial \Xi_{1m}}{\partial \zeta} \, \mathrm{d}\zeta,$$

$$[K_{NL}]_{(2N+j,5N+m)} = \frac{b_{11}}{\eta} \int_0^{\zeta_0} \frac{\partial w_1}{\partial \zeta} \frac{\partial \Xi_{5j}}{\partial \zeta} \frac{\partial \Xi_{1m}}{\partial \zeta} \, \mathrm{d}\zeta, \quad [K_{NL1}]_{(3N+j,3N+m)} = 0,$$

$$[K_{NL1}]_{(3N+j,4N+m)} = \frac{b_{11}}{\eta} \int_0^{\zeta_0} \frac{\partial w_1}{\partial \zeta} \frac{\partial \Xi_{4j}}{\partial \zeta} \frac{\partial \Xi_{2m}}{\partial \zeta} \, \mathrm{d}\zeta,$$

$$[K_{NL1}]_{(3N+j,5N+m)} = \frac{b_{11}}{\eta} \left(\int_{\zeta_0}^{1} \frac{\partial w_2}{\partial \zeta} \frac{\partial \Xi_{7j}}{\partial \zeta} \frac{\partial \Xi_{3m}}{\partial \zeta} \, \mathrm{d}\zeta + \int_0^{\zeta_0} \frac{\partial w_1}{\partial \zeta} \frac{\partial \Xi_{5j}}{\partial \zeta} \frac{\partial \Xi_{2m}}{\partial \zeta} \, \mathrm{d}\zeta \right),$$

$$[K_{NL1}]_{(4N+j,4N+m)} = [K_{NL1}]_{(4N+j,5N+m)} = 0, \quad [K_{NL2}]_{(5N+j,5N+m)} = 0,$$

$$[K_{NL2}]_{(j,m)} = [K_{NL2}]_{(j,N+m)} = [K_{NL2}]_{(j,m)} = [K_{NL2}]_{(j,N+m)} = [K_{NL2}]_{(j,4N+m)} = [K_{NL2}]_{(j,5N+m)} = 0,$$

$$[K_{NL2}]_{(N+j,N+m)} = [K_{NL2}]_{(N+j,m)} = [K_{NL2}]_{(N+j,N+m)} = [K_{NL2}]_{(N+j,4N+m)} = [K_{NL2}]_{(N+j,5N+m)} = 0,$$

$$[K_{NL2}]_{(2N+j,2N+m)} = \frac{3a_{11}}{2\eta^2} \int_0^{\zeta_0} \left(\frac{\partial w_1}{\partial \zeta} \right)^2 \frac{\partial \Xi_{1j}}{\partial \zeta} \frac{\partial \Xi_{1m}}{\partial \zeta} \, \mathrm{d}\zeta, \quad [K_{NL2}]_{(2N+j,3N+m)} = \frac{3a_{11}}{2\eta^2} \int_0^{\zeta_0} \left(\frac{\partial w_1}{\partial \zeta} \right)^2 \frac{\partial \Xi_{2j}}{\partial \zeta} \frac{\partial \Xi_{1m}}{\partial \zeta} \, \mathrm{d}\zeta,$$

$$[K_{NL2}]_{(2N+j,4N+m)} = [K_{NL2}]_{(2N+j,5N+m)} = 0,$$

$$[K_{NL2}]_{(3N+j,3N+m)} = \frac{3a_{11}}{2\eta^2} \left[\int_{\zeta_0}^{1} \left(\frac{\partial w_2}{\partial \zeta} \right)^2 \frac{\partial \Xi_{3j}}{\partial \zeta} \frac{\partial \Xi_{3m}}{\partial \zeta} \, \mathrm{d}\zeta + \int_0^{\zeta_0} \left(\frac{\partial w_1}{\partial \zeta} \right)^2 \frac{\partial \Xi_{2j}}{\partial \zeta} \frac{\partial \Xi_{2m}}{\partial \zeta} \, \mathrm{d}\zeta \right],$$

$$[K_{NL2}]_{(3N+j,4N+m)} = [K_{NL2}]_{(3N+j,5N+m)} = 0, \quad [K_{NL2}]_{(4N+j,4N+m)} = [K_{NL2}]_{(4N+j,5N+m)} = 0, \quad [K_{NL2}]_{(5N+j,5N+m)} = 0,$$

where $j, m = 1, 2, \ldots, N$.

Appendix B

For a cracked FGM beam, the nonlinear governing equations of motion can be derived from Hamilton's principle as

$$A_{11}\left(\frac{\partial^2 U_i}{\partial x^2}+\frac{\partial W_i}{\partial x}\frac{\partial^2 W_i}{\partial x^2}\right)+B_{11}\frac{\partial^2 \Psi_i}{\partial x^2}=I_1\frac{\partial^2 U_i}{\partial t^2}+I_2\frac{\partial^2 \Psi_i}{\partial t^2}, \tag{B.1}$$

$$\kappa A_{55}\left(\frac{\partial^2 W_i}{\partial x^2}+\frac{\partial \Psi_i}{\partial x}\right)+\frac{\partial}{\partial x}\left[N_{xi}\frac{\partial W_i}{\partial x}\right]=I_1\frac{\partial^2 W_i}{\partial t^2}, \tag{B.2}$$

$$B_{11}\left(\frac{\partial^2 U_i}{\partial x^2}+\frac{\partial W_i}{\partial x}\frac{\partial^2 W_i}{\partial x^2}\right)+D_{11}\frac{\partial^2 \Psi_i}{\partial x^2}-\kappa A_{55}\left(\frac{\partial W_i}{\partial x}+\Psi_i\right)=I_2\frac{\partial^2 U_i}{\partial t^2}+I_3\frac{\partial^2 \Psi_i}{\partial t^2}, \tag{B.3}$$

where the subscript $i=1$ and 2 refer to the left sub-beam and right sub-beam divided by the crack; The normal resultant force N_{xi}, bending moment M_{xi}, and transverse shear force Q_{xi} are calculated from

$$N_{xi}=A_{11}\left[\frac{\partial U_i}{\partial x}+\frac{1}{2}\left(\frac{\partial W_i}{\partial x}\right)^2\right]+B_{11}\frac{\partial \Psi_i}{\partial x}, \tag{B.4}$$

$$M_{xi}=B_{11}\left[\frac{\partial U_i}{\partial x}+\frac{1}{2}\left(\frac{\partial W_i}{\partial x}\right)^2\right]+D_{11}\frac{\partial \Psi_i}{\partial x}, \tag{B.5}$$

$$Q_{xi}=\kappa A_{55}\left(\frac{\partial W_i}{\partial x}+\Psi_i\right). \tag{B.6}$$

The corresponding boundary conditions at beam ends ($x=0,L$) require

$$x=0:\ \ U_1=0\ \text{ or }\ N_{x1}=0,\quad W_1=0\ \text{ or }\ Q_{x1}=0,\quad \Psi_1=0\ \text{ or }\ M_{x1}=0, \tag{B.7}$$

$$x=L:\ \ U_2=0\ \text{ or }\ N_{x2}=0,\quad W_2=0\ \text{ or }\ Q_{x2}=0,\quad \Psi_2=0\ \text{ or }\ M_{x2}=0, \tag{B.8}$$

and the compatibility conditions at the cracked section $x=L_1$ are

$$U_1=U_2,\quad W_1=W_2,\quad K_T(\Psi_2-\Psi_1)=M_1,\quad N_{x1}=N_{x2},\quad M_{x1}=M_{x2},\quad Q_{x1}=Q_{x2}. \tag{B.9}$$

The nonlinear frequency of the cracked FGM beams can be obtained by solving Eqs. (B.1)–(B.3) and (B.7)–(B.9). For details of DQM procedure, please refer to Refs. [33,34].

References

[1] P.F. Rizos, N. Aspragathos, A.D. Dimarogonas, Identification of crack location and magnitude in a cantilever beam from the vibration modes, *Journal of Sound and Vibration* 138 (1990) 381–388.
[2] M.H.H. Shen, C. Pierre, Natural modes of Bernoulli–Euler beams with symmetric cracks, *Journal of Sound and Vibration* 138 (1990) 115–134.
[3] M. Krawczuk, W.M. Ostachowicz, Modelling and vibration analysis of a cantilever composite beam with a transverse open crack, *Journal of Sound and Vibration* 183 (1995) 69–89.
[4] B.P. Nandwana, S.K. Maiti, Modelling of vibration of beam in presence of inclined edge or internal crack for its possible detection based on frequency measurements, *Engineering Fracture Mechanics* 58 (1997) 193–205.
[5] M. Chati, R. Rand, S. Mukherjee, Modal analysis of a cracked beam, *Journal of Sound and Vibration* 207 (1997) 249–270.
[6] A.D. Dimarogonas, Vibration of cracked structures: a state of the art review, *Engineering Fracture Mechanics* 55 (1996) 831–857.
[7] B.P. Nandwana, S.K. Maiti, Detection of the location and size of a crack in stepped cantilever beams based on measurements of natural frequencies, *Journal of Sound and Vibration* 203 (1997) 435–446.
[8] T. Yokoyama, M.C. Chen, Vibration analysis of edge-cracked beams using a line–spring model, *Engineering Fracture Mechanics* 59 (1998) 403–409.
[9] T.G. Chondros, A.D. Dimarogonas, J. Yao, A continuous cracked beam vibration theory, *Journal of Sound and Vibration* 215 (1998) 17–34.

[10] M. Kisa, J. Brandon, M. Topcu, Free vibration analysis of cracked beams by a combination of finite elements and component mode synthesis methods, *Computers & Structures* 67 (1998) 215–223.
[11] I. Takahashi, Vibration and stability of non-uniform cracked Timoshenko beam subjected to follower force, *Composite Structures* 71 (1999) 585–591.
[12] M.H. Hsu, Vibration analysis of edge-cracked beam on elastic foundation with axial loading using the differential quadrature method, *Computer Methods in Applied Mechanics and Engineering* 194 (2005) 1–17.
[13] H.P. Lin, S.C. Chang, Forced responses of cracked cantilever beams subjected to a concentrated moving load, *International Journal of Mechanical Sciences* 48 (2006) 1456–1463.
[14] J.A. Loya, L. Rubio, J. Fernández-Sáez, Natural frequencies for bending vibrations of Timoshenko cracked beams, *Journal of Sound and Vibration* 290 (2006) 640–653.
[15] M. Kisa, M.A. Gurel, Free vibration analysis of uniform and stepped cracked beams with circular cross sections, *International Journal of Engineering Science* 45 (2007) 364–380.
[16] K. Aydin, Vibratory characteristics of axially loaded Timoshenko beams with arbitrary number of cracks, *Journal of Vibration and Acoustics* 129 (2007) 341–354.
[17] K. Aydin, Vibratory characteristics of Euler–Bernoulli beams with an arbitrary number of cracks subjected to axial load, *Journal of Vibration and Control* 14 (2008) 485–510.
[18] H.P. Lee, S.P. Lim, Vibration of cracked rectangular plates including transverse shear deformation and rotary inertia, *Composite Structures* 49 (1993) 715–718.
[19] S.E. Khadem, M. Rezaee, Introduction of modified comparison functions for vibration analysis of a rectangular cracked plate, *Journal of Sound and Vibration* 236 (2000) 245–258.
[20] S.E. Khadem, M. Rezaee, An analytical approach for obtaining the location and depth of an all-over part-through crack on externally in-plane loaded rectangular plate using vibration analysis, *Journal of Sound and Vibration* 230 (2000) 291–308.
[21] E. Douka, S. Loutridis, A. Trochidis, Crack identification in plates using wavelet analysis, *Journal of Sound and Vibration* 270 (2004) 279–295.
[22] L.J. Hadjileontiadis, E. Douka, Kurtosis analysis for crack detection in thin isotropic rectangular plates, *Engineering Structures* 29 (2007) 2353–2364.
[23] M. Rucka, K. Wilde, Application of continuous wavelet transform in vibration based damage detection method for beams and plates, *Journal of Sound and Vibration* 297 (2006) 536–550.
[24] A. Demir, V. Mermertas, Natural frequencies of annular plates with circumferential cracks by means of sector element, *Engineering Fracture Mechanics* 75 (2008) 1143–1155.
[25] K. El Bikri, R. Benamar, M.M. Bennouna, Geometrically non-linear free vibrations of clamped–clamped beams with an edge crack, *Computers & Structures* 84 (2006) 485–502.
[26] G.Y. Wu, Y.S. Shih, Dynamic instability of rectangular plate with an edge crack, *Composite Structures* 84 (2005) 1–10.
[27] J.N. Reddy, Z.Q. Cheng, Frequency of functionally graded plates with three-dimensional asymptotic approach, *Journal of Engineering Mechanics* 129 (2003) 896–900.
[28] C.F. Lü, W.Q. Chen, Free vibration of orthotropic functionally graded beams with various end conditions, *Structural Engineering and Mechanics* 13 (2005) 1430–1437.
[29] S. Kitipornchai, J. Yang, K.M. Liew, Random vibration of functionally graded laminates in thermal environments, *Computer Methods in Applied Mechanics and Engineering* 195 (2005) 1075–1095.
[30] M. Aydogdu, V. Taskin, Free vibration analysis of functionally graded beams with simply supported edges, *Materials and Design* 28 (2007) 1651–1656.
[31] H. Matsunaga, Free vibration and stability of functionally graded shallow shells according to a 2D higher-order deformation theory, *Composite Structures* 84 (2008) 132–146.
[32] G.N. Praveen, J.N. Reddy, Nonlinear transient thermoelastic analysis of functionally graded ceramic–metal plates, *International Journal of Solids and Structures* 35 (1998) 4457–4476.
[33] J. Yang, S. Kitipornchai, K.M. Liew, Large amplitude vibration of thermo-electro-mechanically stressed FGM laminated plates, *Computer Methods in Applied Mechanics and Engineering* 192 (2003) 3861–3885.
[34] S. Kitipornchai, J. Yang, K.M. Liew, Semi-analytical solution for nonlinear vibration of laminated FGM plates with geometric imperfections, *International Journal of Solids and Structures* 41 (2004) 2235–2257.
[35] C.S. Chen, Nonlinear vibration of a shear deformable functionally graded plate, *Composite Structures* 68 (2005) 295–302.
[36] J. Woo, S.A. Meguid, L.S. Ong, Nonlinear free vibration behavior of functionally graded plates, *Journal of Sound and Vibration* 289 (2006) 595–611.
[37] A. Allahverdizadeh, M.H. Naei, M. Nikkhah Bahrami, Nonlinear free and forced vibration analysis of thin circular functionally graded plates, *Journal of Sound and Vibration* 310 (2008) 966–984.
[38] R. Sridhar, A. Chakraborty, S. Gopalakrishnan, Wave propagation analysis in anisotropic and inhomogeneous uncracked and cracked structures using pseudospectral finite element method, *International Journal of Solids and Structures* 43 (2006) 4997–5031.
[39] V. Briman, L.W. Byrd, Vibration of damaged cantilevered beams manufactured from functionally graded materials, *AIAA Journal* 45 (2007) 2747–2757.
[40] J. Yang, Y. Chen, Free vibration and buckling analyses of functionally graded beams with edge cracks, *Composite Structures* 83 (2008) 48–60.
[41] J. Yang, Y. Chen, Y. Xiang, X.L. Jia, Free and forced vibration of cracked inhomogeneous beams under an axial force and a moving load, *Journal of Sound and Vibration* 312 (2008) 166–181.

[42] L.L. Ke, J. Yang, S. Kitipornchai, Y. Xiang, Flexural vibration and elastic buckling of a cracked Timoshenko beam made of functionally graded materials, *Mechanics of Advanced Materials and Structures*, 2008, in press.
[43] F. Erdogan, B.H. Wu, The surface crack problem for a plate with functionally graded properties, *Journal of Applied Mechanics* 64 (1997) 448–456.
[44] D. Broek, *Elementary Engineering Fracture Mechanics*, Martinus Nijhoff Publishers, Dordrecht, 1986.
[45] G.H. Su, Y. Xiang, A non-discrete approach for analysis of plates with multiple subdomains, *Engineering Structures* 24 (2002) 563–575.
[46] K.M. Liew, C.M. Wang, Y. Xiang, S. Kitipornchai, *Vibration of Mindlin Plates: Programming the p-version Ritz Method*, Elsevier Science, Oxford, UK, 1998.
[47] G. Singh, G.V. Rao, Nonlinear oscillations of thick asymmetric cross-ply beams, *Acta Mechanics* 127 (1998) 135–146.
[48] G. Singh, G.V. Rao, Analysis of the nonlinear vibrations of unsymmetrically laminated composite beams, *AIAA Journal* 29 (1991) 1727–1735.
[49] S.R. Marur, G. Prathap, Non-linear beam vibration problems and simplifications in finite element models, *Computational Mechanics* 35 (2005) 352–360.